The Journal of Neuroscience
July 1986, 6(7): 1866-1875

Characteristics and Distribution of High- and Low-Affinity Alpha Bungarotoxin Binding Sites in the Rat Hypothalamus

R. B. Meeker, K. M. Michels, M. T. Libber, and J. N. Hayward

Department of Neurology and Neurobiology Curriculum, University of North Carolina, Chapel Hill, North Carolina 27514

When binding of ^{125}I-alpha bungarotoxin (^{125}I-αBTX) to hypothalamic membranes is observed over a wide range of concentrations, 3 binding sites can be identified, with estimated equilibrium dissociation constants (K_ds) of 4.1 × 10^{-11} M, 6.2 × 10^{-10} M, and 9.1 × 10^{-7} M for high-, low-, and very-low-affinity interactions, respectively. The densities of the high- and low-affinity sites were similar at 14-21 fmol/mg protein, whereas the very-low-affinity site had approximately 1000× greater capacity. Association and dissociation kinetics predicted a biphasic binding reaction, with association rate constants of 1.38 × 10^8 M^{-1} min^{-1} and 7.53 × 10^7 M^{-1} min^{-1} and dissociation rate constants of 5.23 × 10^{-3} min^{-1} and 1.80 × 10^{-3} min^{-1}. The presence of Na^+ inhibited the binding of ^{125}I-αBTX with a half-maximally effective concentration of 22 mM. This decrease in binding was associated with the observation of a single binding site with a K_d of 4.3 × 10^{-10} M and a density of 12.1 fmol/mg protein. In competition binding experiments, αBTX, curare, nicotine, and quinacrine were the most potent competitors. Acetylcholine competed with ^{125}I-αBTX binding at 2 sites with estimated affinities of 3.6 × 10^{-8} and 7.4 × 10^{-5} M. In the rostral hypothalamus, high-affinity binding of ^{125}I-αBTX was localized to the region of the supraoptic nucleus, paraventricular nucleus, suprachiasmatic nucleus, and the nucleus circularis complex. Within magnocellular regions, binding was closely associated with neurophysin-immunoreactive neurons and processes, while in the region of the suprachiasmatic nucleus, the binding was in a perinuclear region surrounding parvocellular neurophysin-immunoreactive neurons.

It is now well recognized that the central nervous system possesses an alpha bungarotoxin-binding protein that is biochemically and pharmacologically similar to the nicotinic acetylcholine receptor (nAChR) of electric eel and muscle (Conti-Tronconi et al., 1985; Dolly and Barnard, 1984; Lowy et al., 1976; Morley, 1981; Oswald and Freeman, 1981). The binding of ^{125}I-alpha-bungarotoxin (^{125}I-αBTX) shows selectivity for ACh-sensitive neurons *in vitro* (Carbonetto et al., 1978; Chalazonitis et al., 1974; Greene et al., 1973), is associated with synaptosomes (Salvaterra et al., 1975) and can be localized to the postsynaptic region (Hunt and Schmidt, 1978a; Lentz and Chester, 1977; Marshall, 1981; Smolen, 1983; Vogel et al., 1977). A reliable pattern of ^{125}I-αBTX binding has been observed in the brain, the highest overall concentration of sites generally being in the hypothalamus (Hunt and Schmidt, 1978b; Marks and Collins, 1982; Morley et al., 1977; Segal et al., 1978). Various affinities for the binding of ^{125}I-αBTX to brain membranes have been reported; they range from equilibrium (or kinetic) dissociation constants (K_d) as low as 0.4–3 × 10^{-10} M (Lukas, 1984b; Marks and Collins, 1982; Morley et al., 1977; Salvaterra and Mahler, 1976; Schmidt, 1977; Wang et al., 1978) to intermediate values of 1–5 × 10^{-9} M (Lukas, 1984a, b; Patrick and Stallcup, 1977a; Salvaterra et al., 1975), and finally to the high values of 1–40 × 10^{-8} M (Lukas, 1984b; Salvaterra, et al., 1975). Each of these sites has nAChR-like pharmacology. Given these results, it is not surprising that several investigators have suggested the presence of multiple binding sites for ^{125}I-αBTX in the central nervous system (Lukas, 1984b; Morley et al., 1983; Schmidt, 1977).

The above data from binding analyses provide a striking contrast to those experiments in which αBTX has been unable to block the functional activation of the nAChR in spinal cord (Duggan et al., 1976), sympathetic ganglion (Chou and Lee, 1969), and PC12 cells (Patrick and Stallcup, 1977b). Efforts to clarify such discrepancies by precipitating the ^{125}I-αBTX-binding protein with monoclonal antibodies to the purified nAChR have yielded mixed results, with some investigators successfully immunoprecipitating the ^{125}I-αBTX-binding protein (Block and Billiar, 1979; Dolly and Barnard, 1984), while others have been unsuccessful (Patrick and Stallcup, 1977b). Thus, the precise identity of the αBTX-binding protein remains questionable. This issue is particularly important for the understanding of the role of the cholinergic network which is thought to control the release of vasopressin or oxytocin. The release of vasopressin is well recognized as being induced by nicotinic cholinergic agonists (Volle and Koelle, 1975), and the system that mediates this response is probably contained within the rostral hypothalamus (Sladek, 1983). Further support for this possibility is provided by the high binding of ^{125}I-αBTX in the hypothalamus (Marks and Collins, 1982; Morley et al., 1977; Segal et al., 1978) and particularly the supraoptic nucleus (NSO) of the hypothalamus (Hunt and Schmidt, 1978b; Polz-Tejera et al., 1975; Silver and Billiar, 1976). Electrophysiological evidence indicates that the cells responsive to nicotinic cholinergic agonists may be the same as or similar to the cells that synthesize vasopressin in the NSO of the hypothalamus (Arnauld et al., 1983; Barker et al., 1971; Bioulac et al., 1978; Gahwiler and Dreifuss, 1980; Sakai et al., 1974). Thus, a nicotinic cholinergic synapse within the NSO may be an important link in the neural mechanisms that control the secretion of vasopressin.

In an effort to evaluate the significance of the binding of ^{125}I-αBTX in the NSO and the possible presence of nAChRs, we have characterized pharmacologically the binding of ^{125}I-αBTX in the hypothalamus. A procedure for combining receptor autoradiography and immunocytochemistry on a single free-floating section allowed assessment of the codistribution of neuro-

Received June 27, 1985; revised Nov. 15, 1985; accepted Dec. 30, 1985.

This research was supported, in part, by NIH Javits Award NS-13411, USPHS GRSA FR-05406, a Neurobiology Training Grant, a UNC Faculty Development Award, and a UNC Medical Faculty Grant. The authors wish to express their sincere thanks to Ms. Donna Cronce for her valuable assistance in the development of techniques and the collection of data for these experiments. A preliminary report of portions of this work has been presented (Meeker et al., 1984).

Correspondence should be sent to Dr. R. B. Meeker, Department of Neurology, 781 Clinical Sciences Building 229H, University of North Carolina, Chapel Hill, NC 27514.

physin-immunoreactive neurons and αBTX binding sites.

Three ^{125}I-αBTX binding sites, with K_ds ranging from 4.1×10^{-11} to 4.0×10^{-7} M, can be discriminated in the brain. The high-affinity sites have nicotinic cholinergic pharmacology, a half-time on the receptor of 2–6 hr, and are sensitive to the cation concentration in the buffer. These high-affinity sites are localized to the region of the NSO, suprachiasmatic nucleus (NSC), paraventricular nucleus (NPV), and nucleus circularis (NC). A high correlation of this binding distribution with neurophysin-immunoreactive magnocellular neurons suggests that these binding sites may have a special relevance for the functional organization of the vasopressin/oxytocin neurosecretory system.

Materials and Methods

Materials

Monoiodinated ^{125}I-αBTX was obtained from New England Nuclear at an initial specific activity of 16.5–17.6 μCi/μg (261–279 cpm/fmol). All cholinergic ligands were obtained from Sigma. Normal goat serum was purchased from Antibodies Incorporated. Tetramethylrhodamine isothiocyanate-conjugated goat anti-rabbit IgG (TRITC-GAR, lot no. 15967) was purchased from Cappel. The specific RN4 neurophysin antibody (Reaves et al., 1983; Sokol et al., 1976) was the generous gift of Dr. Alan Robinson, University of Pittsburgh (Grant AM-16166). Other materials were of reagent or comparable quality and were from standard sources.

Preparation of membranes for ^{125}I-αBTX binding

Male Sprague-Dawley rats were lightly anesthetized with sodium pentobarbital (30 mg/kg). Each rat was then killed by decapitation; the brain was rapidly removed and immersed in ice-cold 0.32 M sucrose. The hypothalamus and brain stem were dissected from the brain on ice (Hayward et al., 1983). Washed membranes from each region were prepared by homogenizing the tissue in 10 vol of 0.32 M sucrose. The resulting homogenate was centrifuged at 600 × *g* for 10 min, the pellet discarded, the membrane suspension diluted to a volume of 40 ml with assay buffer (10 mM phosphate buffer, 1 mM EDTA, 0.1 mM phenylethylsulfonyl flouride, 0.02% sodium azide) and centrifuged at 39,000 × *g* for 20 min. The resulting pellet was resuspended in 40 ml assay buffer and again centrifuged at 39,000 × *g*. After a total of 3 washes, the tissue was resuspended in assay buffer at a concentration of 100–200 mg/ml and aliquots stored frozen at −80°C. Binding of ^{125}I-αBTX to the frozen membranes did not differ from that to fresh tissue, and remained stable for at least 1 month.

Characterization of ^{125}I-αBTX binding

Washed membranes were diluted in assay buffer at concentrations ranging from 5 to 50 mg wet wt/ml. A 400 μl aliquot of membranes (2–20 mg wet weight) was added to polypropylene tubes containing 6–1000 pM ^{125}I-αBTX and an appropriate concentration of competing drug or buffer. Final assay volume was 0.5 ml. Tubes were incubated at 22°C for 2.5 hr. The reaction was terminated by adding 10 ml of wash buffer (10 mM phosphate-buffered saline, 0.5% gelatin, pH 7.4), followed by rapid filtration through Schleicher and Schuell no. 30 glass fiber filters. Each filter was washed twice with 100 ml of wash buffer. The dry filters were transferred to 13 × 100 mm tubes and counted in a Tracor gamma counter at an efficiency of 85–90%. This procedure was effective in reducing any nonspecific binding of ^{125}I-αBTX to the glass fiber filters to less than 1% of the total counts added at the highest ligand concentrations. These filter blanks were constant within each experiment and were subtracted from the total binding values. Attempts to reduce nonspecific filter binding with other compounds, including serum albumins, poly-L-lysine, 0.5 M NaCl, and Prosil (Harden et al., 1983), were less effective. Nonspecific binding to tissue ranged from 10 to 50% of the total binding, depending on the concentration of ^{125}I-αBTX in the assay. Both total and nonspecific binding of ^{125}I-αBTX to rat brain membranes were found to be unaffected by pH in the range of 7.0–8.2. Results obtained with the filtration binding assay were the same as those of experiments utilizing a centrifugation assay protocol. Protein determinations were made on samples of the tissue homogenates according to the method of Lowry et al. (1951).

A protocol similar to the above was followed for the binding of ^{125}I-αBTX to 50 μm sections of hypothalamus, with the following exceptions: (1) Sections were washed in an excess of assay buffer and then transferred to a 24-well tissue culture plate containing ^{125}I-αBTX in a final assay volume of 1 ml. (2) Binding was terminated by transferring the sections through 3 successive 2 min washes in 2 ml of wash buffer and, finally, into a 13 × 100 mm test tube containing 0.5 ml assay buffer. Each section was immediately counted for 1 min in a Tracor gamma counter and then quickly mounted onto a gelatin–chrome alum-coated glass slide and dried in preparation for autoradiography.

Data analysis

Computer analysis of the data from saturation binding and competition binding experiments was accomplished by using either a Gauss-Newton or Marquart nonlinear least-squares regression program that required a minimum of approximately 15 data points per curve. Since highly accurate values are difficult to obtain with nonspecific binding and other potential sources of variability exceeding 10% of the total binding, such values should be considered estimates, particularly for the low-affinity site. Error values for replicate determinations of K_ds were ±31% and ±102% for the high- and low-affinity sites, respectively. Estimates for both the high- and low-affinity B_{max} values were replicated to within ±17%. The saturation binding nonlinear regression was based on the equation,

$$B = \frac{B_{max1} \times L}{L + K_{d1}} + \frac{B_{max2} \times L}{L \times K_{d2}}$$

where B = total ligand specifically bound, L = ligand concentration, K_{d1} = dissociation constant for the high-affinity site, B_{max1} = density of the high-affinity site, K_{d2} = dissociation constant for the low-affinity site, and B_{max2} = density of the low-affinity site.

Competition binding nonlinear regression analysis was based on the equation,

$$\text{Fractional occupancy} = \frac{B_{max1}}{B_T} \times \frac{L}{L + IC_{50,1}} + \frac{B_{max2}}{B_T} \times \frac{L}{L + IC_{50,2}}$$

where B_T = total ligand bound, L = ligand concentration, $IC_{50,1}$ = concentration of drug that inhibits half the high-affinity binding, $IC_{50,2}$ = concentration of drug that inhibits half the low-affinity binding, B_{max1} = relative density of high-affinity sites, and B_{max2} = relative density of low-affinity sites.

Inhibition constants (K_Is) from competition binding experiments were calculated from IC_{50} values according to Cheng and Prusoff (1973):

$$K_I = \frac{IC_{50}}{1 + F/K_d}$$

where IC_{50} = the concentration of drug that inhibits half the ligand binding, F = the free molar concentration of the ligand, and K_d = the dissociation constant of the ligand. Conditions for competition binding were generally established such that the majority of the ligand binding was to the high-affinity site. Consequently, the high-affinity K_d estimates were used for the calculation of the inhibition constants.

Combined receptor autoradiography and neurophysin immunocytochemistry

Male Sprague-Dawley rats were deeply anesthetized with sodium pentobarbital (60 mg/kg). The chest cavity was opened and the rat was rapidly perfused through the heart with a balanced salt solution (50 ml) followed by 0.5% paraformaldehyde in 50 mM PBS (200 ml, pH 7.4). The brain was removed, blocked, and postfixed overnight at 22°C in the same 0.5% paraformaldehyde solution. Free-floating 50 μm sections were cut on a vibrating microtome and then processed sequentially through the following solutions: (1) 0.01 mM PBS, pH 7.4, 5 min × 2, (2) 0.01 M PBS, 1% normal goat serum, 0.01% sodium azide, 10 min, (3) neurophysin antibody RN4 (1:2000), 16–24 hr at 4°C in PBS, 1% normal goat serum, 0.01% sodium azide, (4) 2 ml receptor-binding assay buffer, 5 min at 22°C × 3, (5) 1 ml binding assay buffer containing 10–1000 pM ^{125}I-αBTX and TRITC-GAR (1:200), 2.5 hr at 22°C, and (6) 2 ml PBS, 2 min × 3. At the end of the labeling/binding procedure,

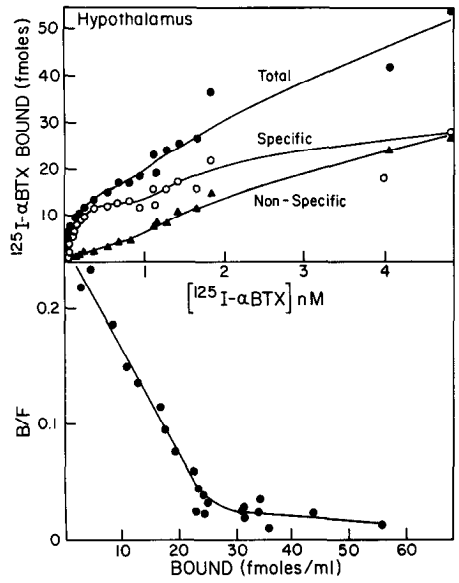

Figure 1. Saturation binding profile for the interaction of ^{125}I-αBTX with fresh, washed membranes from rat hypothalamus. Each assay tube, containing 360 μg tissue protein, was incubated with 13-4852 pM ^{125}I-αBTX for 2.5 hr at 22°C. *Top,* Total (●), specific (○), and nonspecific (▲) binding of ^{125}I-αBTX is plotted as a function of the free ^{125}I-αBTX concentration. Two-site analysis of the Scatchard curve for specific ^{125}I-αBTX binding (*bottom*), using a Gauss-Newton nonlinear regression curve-fitting procedure, resulted in K_d estimates of 4.1×10^{-11} M and 6.2×10^{-10} M for the high- and low-affinity sites, respectively. Estimates of B_{max} were 21.1 and 13.9 fmol/mg protein for the high- and low-affinity sites, respectively. Nonspecific binding was determined in the presence of 10^{-5} M αBTX.

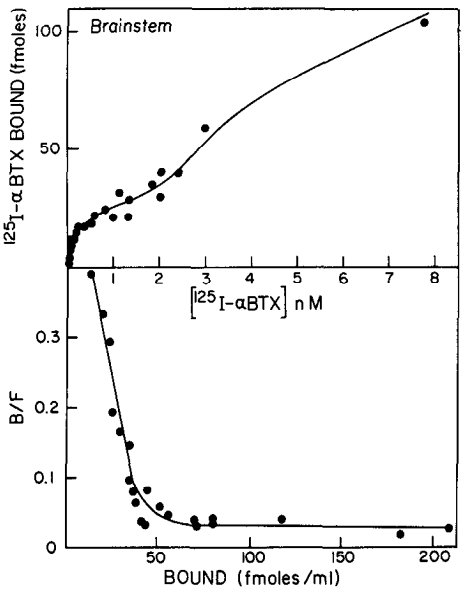

Figure 2. Saturation binding profile for the interaction of ^{125}I-αBTX with washed membranes prepared from rat brain stem. Specific binding of ^{125}I-αBTX to 820 μg tissue protein is plotted as a function of free ligand concentration from 6 to 7721 pM (*top*). Nonlinear regression analysis of the Scatchard curve (*bottom*) resulted in K_d estimates of 2.2×10^{-11} M and 2.8×10^{-9} M for the high- and low-affinity sites, respectively. Estimates of B_{max} were 17.6 and 25.8 fmol/mg protein. Nonspecific binding was determined in the presence of 10 mM ACh.

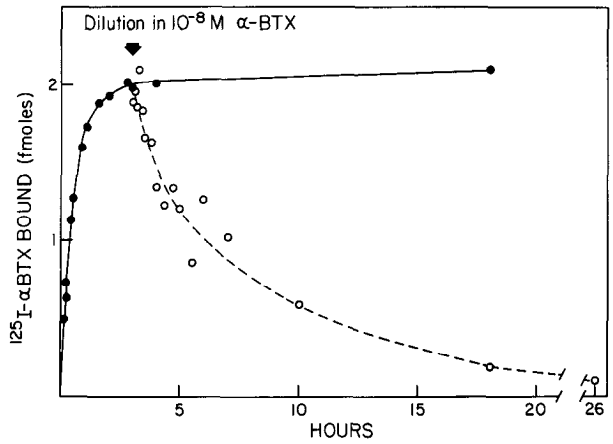

Figure 3. Time course for the association (●) and dissociation (○) of ^{125}I-αBTX on membranes prepared from rat brain. Tissue (338 μg protein) was incubated in 0.5 ml assay buffer containing 182 pM ^{125}I-αBTX for the times indicated. After 3 hr, membranes were diluted in 20-fold excess assay buffer containing 10^{-8} M αBTX. The dissociation process was terminated at the indicated times by rapid filtration and washing of the membranes.

each section was counted and prepared for autoradiography, as described above. Nonspecific binding values determined in the presence of excess *d*-tubocurarine, nicotine, or acetylcholine were all found to give comparable results (approximately 20–40% nonspecific binding). The wet weight of the sections used for this assay averaged 0.580 ± 0.052 mg and contained approximately 52.7 μg of protein.

Autoradiography

Slides containing 50 μm sections of hypothalamus were dipped in Kodak NTB-2 emulsion at 45°C in total darkness. The emulsion-coated slides were allowed to dry at room temperature and were then transferred to sealed, desiccated slide boxes, where they were exposed at 4°C for a period of 14–28 d (2000–4000 cpm × d). At the end of the exposure period, the emulsion was developed in Kodak D-19 (1:1) for 4 min, washed in distilled water for 10 sec, and fixed in Kodak fixer for 5 min. Sections were examined unstained or lightly counterstained in Pyronin Y according to the following procedure: (1) Distilled water, 5 dips. (2) Citric acid–sodium phosphate buffer, 20 mM, pH 5.6, 5 dips. (3) 0.2% Pyronin Y in citrate–phosphate buffer, 5 dips. (4) Citrate–phosphate buffer, 5 dips. (5) Distilled water, 5 dips × 2. The sections were then dehydrated in 50, 70, 80, 95, and 100% ethanol (2 min each), cleared in xylene, and coverslipped with Permount. The distribution of silver grains was examined and photographed on a Leitz Orthoplan microscope under both bright- and dark-field illumination.

Results

Binding of low concentrations of ^{125}I-αBTX to rat brain membranes

Binding of ^{125}I-αBTX to membranes from rat hypothalamus is linear over a range of at least 0.5–0.6 mg protein (data not shown). Saturation binding of ^{125}I-αBTX to hypothalamic membranes is illustrated in Figure 1. The binding profile is complex, appearing to approach saturation at 4×10^{-10} M ^{125}I-αBTX and then increasing again. A Scatchard analysis (Fig. 1, bottom) of the data indicated the presence of 2 binding sites. Nonlinear regression analysis (regression lines not shown) identified a high-affinity ^{125}I-αBTX binding site, with a K_d of 4.1×10^{-11} M and a maximum density (B_{max}) of 21.1 fmol/mg protein, and a low-affinity site with a K_d of 6.2×10^{-10} M and a B_{max} of 13.9 fmol/mg protein.

The characteristics of ^{125}I-αBTX binding to membranes prepared from brain stem, illustrated in Figure 2, are qualitatively and quantitatively similar to those of membranes from hypothalamus. Two-site analysis of the biphasic binding profile predicted K_ds of 2.2×10^{-11} M and 2.8×10^{-9} M for the high- and

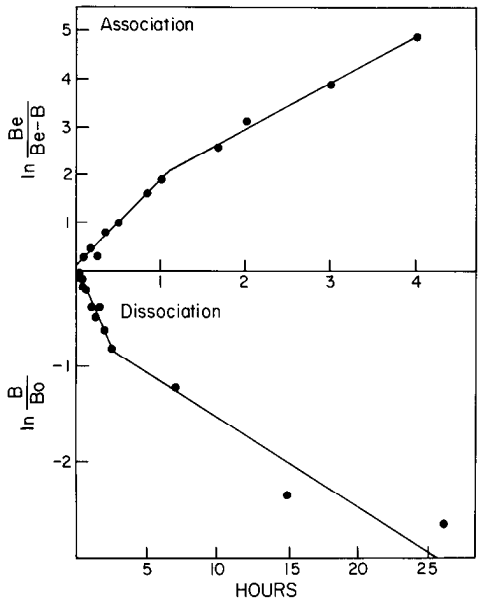

Figure 4. Transformed association and dissociation rate data from Figure 3. *Top,* Natural logarithmic transformation of the amount of ^{125}I-αBTX bound at equilibrium (B_e), divided by the difference between B_e and the amount bound at each time point, B, on the association curve, plotted as a function of time. Approximately 80% of the bound ^{125}I-αBTX associates as a fast component and 20% as a slower component. The estimated association rate constants from the slope of each line are 1.38×10^8 M^{-1} min^{-1} and 7.53×10^7 M^{-1} min^{-1} for the fast and slow components, respectively. *Bottom,* Natural logarithmic transformation of the amount of ^{125}I-αBTX bound at each time point, B, relative to the amount bound at the beginning of the dissociation process (B_0). Approximately 60% of the total bound dissociates as a fast component and 40% as a slow component. Estimates of the dissociation rate constants are 5.23×10^{-3} min^{-1} and 1.80×10^{-3} min^{-1} for the fast and slow components, respectively.

low-affinity sites, respectively, and corresponding densities of 17.6 and 25.8 fmol/mg protein. The presence of both high- and low-affinity binding sites throughout the brain was confirmed by the observation of similar curvilinear binding profiles to the hippocampus, amygdala, septum, and cortex. The regions varied only in the density of binding sites, with the hypothalamus having the highest density. The remaining regions all exhibited similar receptor densities.

Kinetics of ^{125}I-αBTX binding

The association and dissociation of ^{125}I-αBTX on membranes is illustrated in Figure 3. Equilibrium is established after approximately 2.5 hr at 22°C and is maintained for at least 18 hr. Dilution of the membranes in 20-fold excess assay buffer containing 10^{-8} M αBTX to halt the association process initiated a relatively rapid decline in the ^{125}I-αBTX bound to the membranes. Analysis of the transformed data (Fig. 4) indicated the presence of a biphasic rate process for both the association and dissociation of ^{125}I-αBTX. Association rate (k_{+1}) estimates yielded values of 1.38×10^8 M^{-1} min^{-1} and 7.53×10^7 M^{-1} min^{-1} for the fast and slow components, respectively. Analysis of the dissociation process yielded rates of 5.23×10^{-3} min^{-1} and 1.80×10^{-3} min^{-1} for the fast and slow components, respectively ($t_{1/2}$ = 132 and 385 min, respectively). The fast component accounted for the majority of the association (80%), whereas the slow component accounted for approximately 60% of the total dissociation.

Analysis of a very-low-affinity ^{125}I-αBTX binding site

Recently, Lukas (1984b) described a binding site for ^{125}I-αBTX in brain that had a K_d of 4×10^{-7} M. Since a site of such low

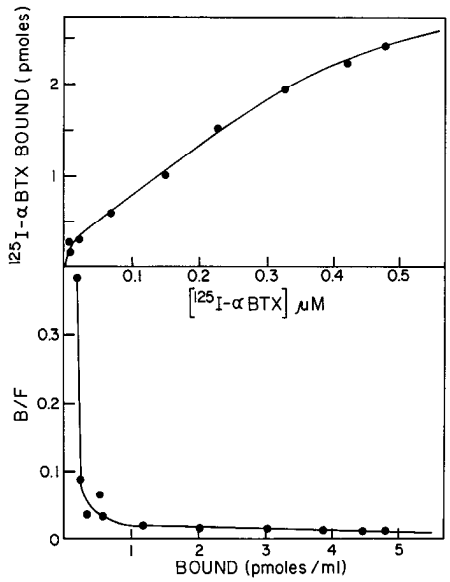

Figure 5. Very-low-affinity binding of ^{125}I-αBTX. *Top,* Saturation binding isotherm for the interaction of 0.54–476 nM ^{125}I-αBTX (2 cpm/fmol) with 240 μg of brain membrane protein. Specific binding is plotted as a function of ^{125}I-αBTX concentration. *Bottom,* Scatchard analysis of the data illustrates binding of ^{125}I-αBTX to 2 sites. The very-low-affinity site has an estimated K_d of 910 nM and a density of 28.1 pmol/mg protein. Nonspecific binding was defined as binding in the presence of 5 mM ACh and varied from 24 to 42% of total binding.

affinity could not be detected using our standard assay conditions, we reduced the specific activity of our ^{125}I-αBTX to 1–2 cpm/fmol by adding unlabeled αBTX. This specific activity was too low to measure the high-affinity binding of ^{125}I-αBTX. A saturation binding analysis (Fig. 5) confirmed the presence of a very-low-affinity binding site with a K_d of 9.1×10^{-7} M and a B_{max} of 28.1 pmol/mg protein. Some binding to the low-affinity ^{125}I-αBTX binding site was also measured under these conditions, yielding a curvilinear Scatchard plot.

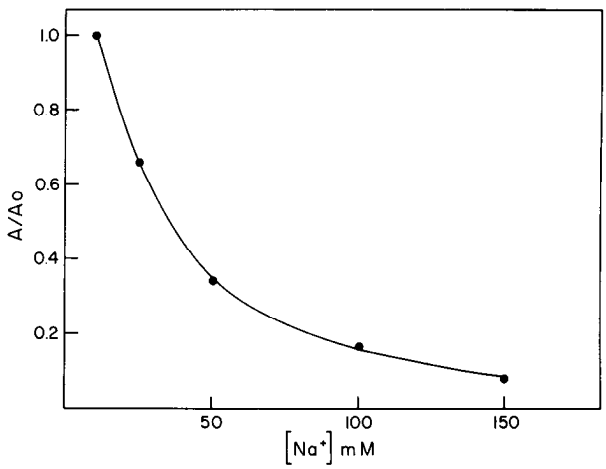

Figure 6. Inhibition of ^{125}I-αBTX binding as a function of increasing concentrations of Na^+ in the assay buffer. Brain membranes (480 μg protein) were incubated in assay buffer containing 157 pM ^{125}I-αBTX and the indicated concentration of Na^+ as the chloride salt. A total of 2.23 fmol of ^{125}I-αBTX was specifically bound in assay buffer (A_0; 10 mM Na^+). The amount of ^{125}I-αBTX specifically bound in the presence of additional Na^+ (A) relative to A_0 is plotted as a function of Na^+ concentration. Nonspecific binding in the presence of 5 mM ACh was 29% and 70% of total binding at 10 and 150 mM Na^+, respectively.

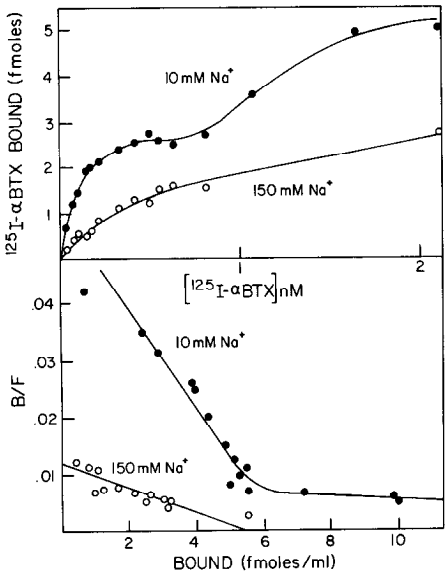

Figure 7. Saturation binding analysis of the interaction of ^{125}I-αBTX with brain membranes in the presence of 150 mM Na^+. A total of 424 μg of tissue protein was incubated with 32–2136 pM ^{125}I-αBTX in assay buffer (●) or assay buffer containing 150 mM Na^+ (○) for 2.5 hr at 22°C. *Top,* Specific binding of ^{125}I-αBTX is plotted as a function of free ^{125}I-αBTX concentration. *Bottom,* Scatchard analysis of the data illustrates 2 binding components in the presence of 10 mM Na^+ and a single binding component in the presence of 150 mM Na^+. Nonspecific binding of ^{125}I-αBTX in the presence of 10 mM ACh ranged from 18% of the total counts bound at low ^{125}I-αBTX concentrations to 49% of the total counts bound at high concentrations.

Effects of Na^+ on ^{125}I-αBTX binding

The presence of increasing concentrations of NaCl in the assay buffer progressively inhibited the binding of ^{125}I-αBTX (Fig. 6) with a half-maximally effective concentration of 22 mM. The effect of Na^+ on the affinity of ^{125}I-αBTX for its binding site is illustrated in Figure 7. In 150 mM Na^+, the specific binding of ^{125}I-αBTX exhibits a saturation binding profile typical of interaction with a single site. Scatchard analysis of the data confirmed the presence of a single site with a K_d of 4.3×10^{-10} M and a maximum density of 12.1 fmol/mg protein, approximately equal to the density (15.2 fmol/mg protein) of the high-affinity site in the presence of 10 mM Na^+.

Comparison of the effects of the chloride salts of other monovalent cations on the binding of ^{125}I-αBTX revealed a similar inhibitory effect. The following order of potency was found, based on the ability to inhibit 50% (IC_{50}) of the total specific ^{125}I-αBTX binding in 10 mM assay buffer: Na^+, NH_4^+, Rb^+ (22–

Table 1. Affinity of various compounds for the αbungarotoxin receptor in rat brain

Drug	K_i (μM)
αBungarotoxin	0.003
d-Tubocurarine	0.117
Nicotine	2.1
Dimethylphenylpiperazinium	2.2
Quinacrine	3.9
Ethopropazine	27.2
Substance P	31.4
Butyrlcholine	88.5
Acetylcholine	93.0
Choline	267
Arginine vasopressin	>10
Phenylmethylsufonylfluoride	>100

The binding of each compound in competition with ^{125}I-αBTX was determined under standard assay conditions at concentrations of 149–459 pM ^{125}I-αBTX. Under such conditions, the number of high-affinity sites occupied, relative to low-affinity sites, is greater than 5:1. Inhibition constants (K_i) were calculated according to Cheng and Prusoff (1973). Binding that could not be inhibited by the drugs represented 24 ± 9% of total binding.

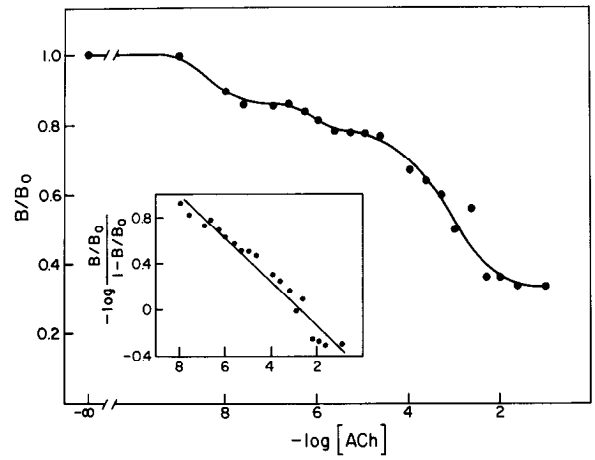

Figure 8. Competition binding curve for ACh in the presence of 517 pM ^{125}I-αBTX. Ligand bound in the presence of varying concentrations of ACh (*B*) relative to the amount bound in the absence of added competitor (B_0; 750 cpm) is plotted as a function of the molar ACh concentration. Hill analysis of the binding data (*inset*) yielded a straight line ($r^2 = 0.96$) with a slope of −0.19. At the highest ACh concentration, 64% of the total binding was displaced. Nonlinear regression analysis of the binding curve indicated the presence of at least 2 binding sites with apparent affinities for ACh of $3.6 \pm 2.8 \times 10^{-8}$ M and $7.4 \pm 0.3 \times 10^{-5}$ M. Binding was accomplished in the presence of 10 μM eserine and 1 μM atropine to minimize degradation of the ACh and interaction with muscarinic receptors, respectively. Data represent the average of 2 experiments. SE for each data point, less than ±12%.

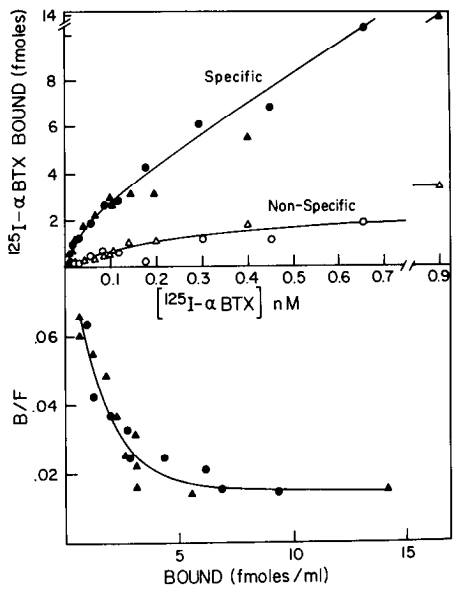

Figure 9. Concentration-dependent accumulation of ^{125}I-αBTX on 50 μm sections of rat hypothalamus. Hypothalamic sections containing approximately 53 μg of protein were incubated in 11–900 pM ^{125}I-αBTX for 2.5 hr at 22°C. The saturation binding (*top*) and Scatchard curves (*bottom*) are the composite of 2 independent experiments (*circles* and *triangles*). Nonspecific binding was measured in the presence of 5 mM ACh.

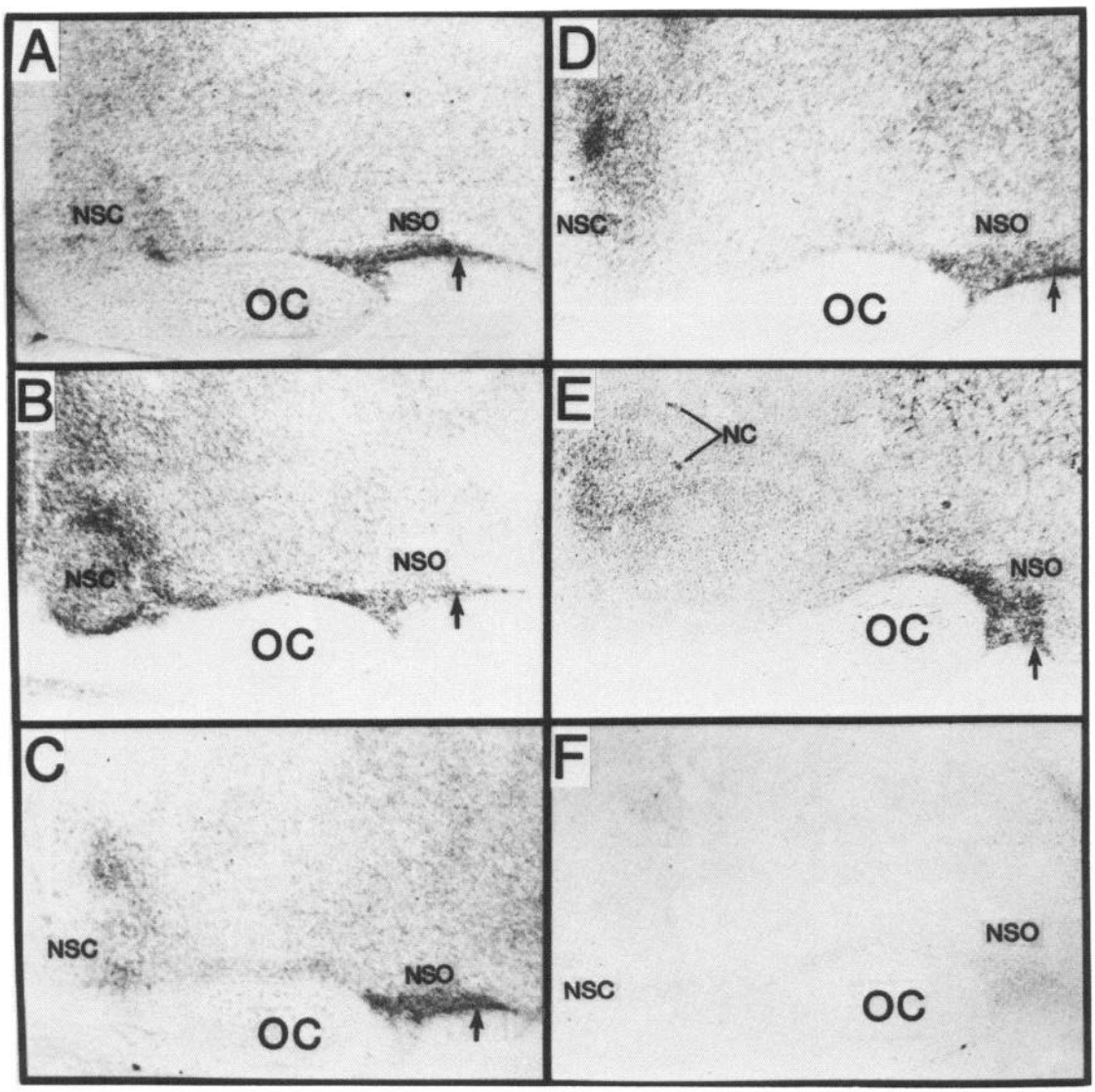

Figure 10. Distribution of high-affinity ^{125}I-αBTX binding sites in the rostral hypothalamus. *A–E,* Bright-field photomicrographs of uncounterstained 50 μm sections illustrating the accumulation of silver grains after incubation in 54–111 pM ^{125}I-αBTX and processing for autoradiography. Sections were sampled at anterior–posterior coordinates of approximately A6400, A6200, A6100, A6000, A5800, and A5900 for *A–F,* respectively, according to the coordinate system of Konig and Klippel (1963). *Arrow,* High density of labeling along the base of the NSO. *F,* Nonspecific binding of ^{125}I-αBTX. The section is lightly counterstained with Pyronin Y to illustrate the location of the various nuclei. Exposure time, 28 d at 4°C. *Magnification,* ~38×. *NSO,* Supraoptic nucleus; *NC,* nucleus circularis complex; *NSC,* suprachiasmatic nucleus; *OC,* optic chiasm.

26 mM) > Li^+ (39 mM) > K^+ (47 mM) > Cs^+ (54 mM). Concentrations of sucrose up to 150 mM had no effect on the binding of ^{125}I-αBTX.

Pharmacology of ^{125}I-αBTX binding

The binding of a variety of ligands in competition with ^{125}I-αBTX is summarized in Table 1. The K_I for each compound was calculated according to Cheng and Prusoff (1973) from the concentration at which half-maximal inhibition of binding occurs (IC_{50}). The most potent competitor was αBTX, followed by *d*-tubocurarine > nicotine, dimethylphenylpiperazinium, and quinacrine > ethopropazine, substance P, butyrlcholine, and acetylcholine > choline, arginine vasopressin, and phenylmethylsulfonyl fluoride. These data must be interpreted cautiously, however, since Hill analyses of the data for ACh, αBTX, *d*-tubocurarine, and dimethylphenylpiperazinium reveal slopes of 0.2–0.5, indicating complex binding interactions. The complexity of the competition binding curve for ACh is illustrated in Figure 8. Hill analysis of the curve (Fig. 8, inset) yielded a slope of 0.2. A nonlinear regression analysis of the data indicates the presence of two binding sites. The high-affinity binding site (estimated $K_I = 3.6 \times 10^{-8}$ M) accounted for 31.4% of the total binding sites. The low-affinity binding site (estimated $K_I = 7.4 \times 10^{-5}$ M) accounted for 68.6% of the total binding sites.

The competition binding of ACh in the presence of 150 mM Na^+, where the ^{125}I-αBTX is interacting with a single site, reduced the complexity of the ACh binding profile. Inhibition of ^{125}I-αBTX binding in the 10^{-8}–10^{-6} M range was lost, yielding a steeper curve with a Hill coefficient of 0.53.

Binding of ^{125}I-αBTX to hypothalamic sections from fixed brain

Saturation binding and kinetic analyses of ^{125}I-αBTX binding to membranes prepared from 0.5% paraformaldehyde-fixed rat brain yielded results similar to those for unfixed membranes. The concentration-dependent accumulation of ^{125}I-αBTX achieved by free-floating 50 μm sections through the rostral hypothalamus of the fixed rat brain is illustrated in Figure 9. A

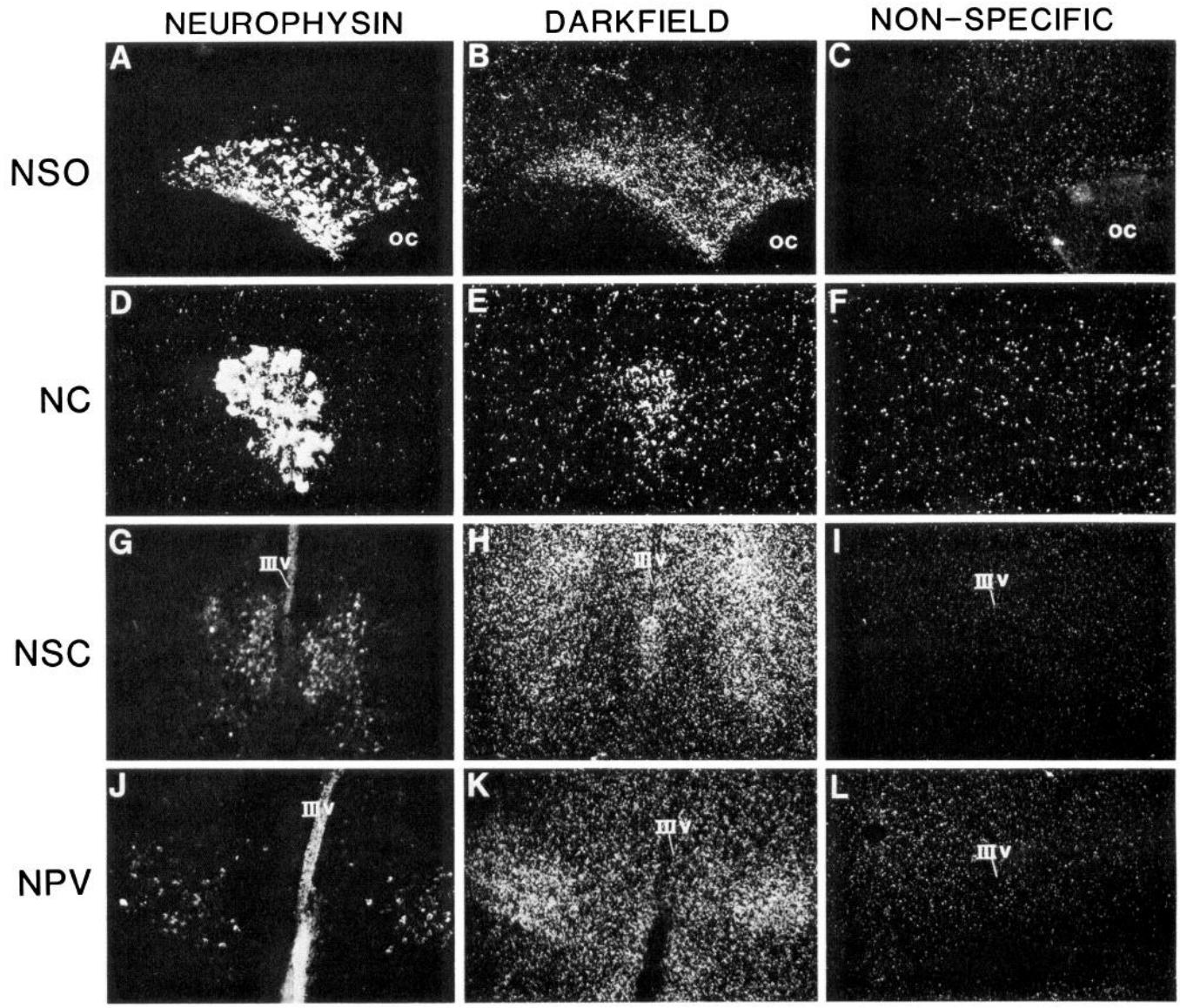

Figure 11. Distribution of ^{125}I-αBTX binding in relation to neurophysin-containing cells of the rostral hypothalamus. Hypothalamic sections were double-labeled by combining neurophysin immunocytochemistry with ^{125}I-αBTX binding under conditions optimal for both. *NSO, NC, NSC,* and *NPV* labeled at ligand concentrations of 103, 73, 29, and 111 pM, respectively. The first pair of photographs for each region (*A–B, D–E, G–H, J–K*) represents the same section under 548 nm incident illumination, for visualization of the TRITC-GAR–neurophysin complex (*A, D, G, J*), or under *dark-field* illumination for visualization of the overlying silver grains (*B, E, H, K*). Nonspecific binding of ^{125}I-αBTX for the same region and concentration was determined on a separate section and is illustrated in the dark-field photomicrographs on the *right* (*C, F, I, L*). Exposure time, 14 d at 4°C. *Magnification,* ~150× for NSO, NC, and NPV; 375× for NSC. *NPV,* Paraventricular nucleus; *IIIV,* third ventricle; other abbreviations as in Figure 10.

Scatchard analysis (Fig. 9, bottom) clearly illustrates the presence of 2 binding components. Dissociation constants of 1.7×10^{-11} and 2.0×10^{-10} M were calculated for the high- and low-affinity interactions, respectively. The density of the high-affinity site was approximately 1.6 fmol/section, while the density of the low-affinity site was approximately 6.1 fmol/section.

Distribution of high-affinity ^{125}I-αBTX binding sites in rat hypothalamus

The hypothalamic distribution of ^{125}I-αBTX binding at concentrations that predominantly label the high-affinity site is shown in Figure 10. The accumulation of ^{125}I-αBTX is highly selective for the region of the NSO, NSC, and the NC. Weaker labeling occurs in the NPV, and some scattered diffuse labeling in the lateral and anterior dorsal hypothalamus. We observed no consistent, anatomically discrete distribution of ^{125}I-αBTX that correlated with low- and very-low-affinity binding sites.

The close association of high-affinity ^{125}I-αBTX binding with neuroendocrine cells is illustrated by the high correlation between the distribution of autoradiographic silver grains and neurophysin-immunoreactive cells on the same section. Examples of the distribution of ^{125}I-αBTX in relation to neurophysin-immunoreactive cells for the NSO, NC, NSC, and NPV are given in Figure 11. Within the NSO (Fig. 11, *A–C*), silver grains were found to be distributed across all neurophysin-immunoreactive cells. The highest density of grains was found to be localized to the ventral dendritic neuropil of the NSO, a region replete with immunofluorescent varicosities thought to be dendrites of the vasopressin and oxytocin magnocellular neurons (Armstrong et al., 1982). Grain density diminished sharply over

the glial cell layer along the basal lamina, in which few or no immunofluorescent varicosities were observed.

The NC (Fig. 11, *D–F*) and magnocellular portions of the posterior lateral, anterior, and periventricular NPV (Fig. 11, *G–I*) were similar to the NSO, with silver grains appearing over the immunofluorescent cell bodies and processes. The density of grains in the core of the NC was as high as in the NSO, whereas the density in the NPV was much less. In contrast to the above, the binding of ^{125}I-αBTX in the NSC did not overlap with the neurophysin-immunoreactive cell bodies (Fig. 11, *G–I*). The perimeter of the NSC was generally labeled, leaving the immunofluorescent cell bodies in the medial portion of the NSC unlabeled.

Discussion

As many as 3 different sites can be identified for the binding of ^{125}I-αBTX to rat hypothalamus and brain stem membranes on the basis of differing affinities and kinetic properties. Each of these sites corresponds to an αBTX binding site that has been described previously. Saturation binding experiments by Schmidt (1977) and kinetically determined affinities by Lukas (1984b) have yielded K_ds of 4–5 × 10^{-11} M. Salvaterra et al. (1975) and Lukas (1984b) have observed both high- and low-affinity binding sites in the same preparations with K_ds of 0.9–5 × 10^{-9} M and 1–40 × 10^{-8} M, respectively, for the high- and low-affinity sites. Other investigators have reported single affinities of 1–5 × 10^{-9} M for the binding of ^{125}I-αBTX to brain membranes (Lukas, 1984a; Patrick and Stallcup, 1977b; Salvaterra et al., 1975). Failure to observe more than one binding site can often be attributed to the use of a restricted range of ligand concentrations or to the cation concentration of the binding buffer.

The significance of each type of ^{125}I-αBTX binding remains to be determined, but a substantial body of existing data indicates that ^{125}I-αBTX binds with high affinity to a nicotinic cholinergic receptor-like polypeptide in rat brain. This binding is (1) on synaptosomes (Salvaterra et al., 1975), (2) associated with a protein with hydrodynamic properties and an isoelectric point similar to *Torpedo* nicotinic receptors (Lowy et al., 1976; Salvaterra and Mahler, 1976), (3) localized to the postsynaptic membrane (Hunt and Schmidt, 1978a; Lentz and Chester, 1977; Smolen, 1983; Vogel et al., 1977), (4) nonuniformly distributed in brain (Hunt and Schmidt, 1978b; Marks and Collins, 1982; Morley et al., 1977; Polz-Tejera et al., 1975; Segal et al., 1978; Silver and Billiar, 1976), and (5) able, in some cases, to be immunoprecipitated by antibodies to the purified nicotinic cholinergic receptor (Block and Billiar, 1979; Conti-Tronconi et al., 1985; Dolly and Barnard, 1984).

The binding of various drugs in competition with ^{125}I-αBTX is also consistent with that expected for a nicotinic cholinergic receptor, with *d*-tubocurarine, nicotine, and dimethylphenylpiperazinium inhibiting the binding of ^{125}I-αBTX at relatively low concentrations. Each compound interacted with both the high- and low-affinity ^{125}I-αBTX binding sites. Inhibition of binding by ACh was particularly complex, as is illustrated by the heterogeneity of the competition curve. The shallow slope of the competition curve indicates that ACh recognizes 2 binding sites, with estimated affinities of 3.6 × 10^{-8} M and 7.4 × 10^{-5} M. Computer analysis of the ACh competition binding curve indicated that 31.4% of the total binding sites corresponded to high-affinity ACh binding, whereas 68.6% of the binding sites were of low affinity. This distribution of high- and low-affinity sites is similar to what would be predicted from the concentration of ^{125}I-αBTX (517 pM) used in the assay, given the K_d values obtained from the Scatchard analysis. Competition binding experiments in the presence of 150 mM Na^+, where only a single ^{125}I-αBTX binding site can be discriminated, eliminated the high-affinity ACh interaction but increased the Hill slope only to a value of 0.53, suggesting that ACh was still interacting at 2 sites. Thus, it would appear that the high-affinity ACh binding may have corresponded to a low-affinity ^{125}I-αBTX binding site and that the heterogeneous ACh binding reflected in the competition curve was not simply a function of the complexity of the ^{125}I-αBTX interaction.

Evidence indicating that several polypeptides in the CNS bind cholinergic ligands and that substantial variation may exist between different types of tissue has been accumulating over the past several years. For example, multiple nicotinic cholinergic-like binding sites have been reported for ^{3}H-nicotine (Romano and Goldstein, 1980), ^{3}H-dihydro-β-erythrodine (Williams and Robinson, 1984), as well as ^{125}I-αBTX (Lukas, 1984b; Salvaterra et al., 1975; Yazulla and Schmidt, 1977). Only a single binding site has been reported for ^{3}H-ACh (Schwartz et al., 1982), but a site with a K_d greater than 10^{-8} M could not have been measured because of high nonspecific binding. More biochemical characterization is needed to clearly evaluate the significance and interrelationships of each of these binding sites. Our data, indicating that ^{125}I-αBTX can bind specifically to 3 different binding sites in rat brain, compare favorably with the observation of Betz et al. (1982) that ^{125}I-αBTX binds to 3 different polypeptides isolated from chick retina. Only 1 of these polypeptides was similar in size to purified nAChR. The protein from rat brain that binds ^{125}I-αBTX can be 75% precipitated by antibodies to muscle nAChR, but not by antibodies to *Torpedo* nAChR (Mills and Wonnacott, 1984). Recently, Conti-Tronconi et al. (1985) have demonstrated an ACh receptor from chick brain that is homologous, but not identical, to the muscle nicotinic ACh receptor.

The binding of ^{125}I-αBTX to rat brain membranes is highly sensitive to the Na^+ concentration in the buffer. The sharp decline in binding as the buffer Na^+ concentration increases appears to be due to a decrease in the affinity of the ^{125}I-αBTX for the high-affinity binding site, and possibly to a loss of the low-affinity binding site. All monovalent cations decrease the binding of ^{125}I-αBTX, indicating a general lack of cation specificity. The order of potency of the various cations does not predict a simple interaction of αBTX with the Na^+ channel. The significance of this cation sensitivity remains to be determined.

To better understand the relationship between the vasopressin/oxytocin neuroendocrine system and its stimulation by putative nicotinic cholinergic input, we have assessed the binding of ^{125}I-αBTX to free-floating sections of 0.5% paraformaldehyde-fixed hypothalamus under conditions that allow double-labeling with an immunocytochemical probe. With this approach, it is clear that high-affinity binding sites for ^{125}I-αBTX are concentrated in the region of the NSO, NC, NPV, and NSC. Of these regions, the NSO contains the most striking concentration of ^{125}I-αBTX binding sites. The binding overlaps greatly with the localization of neurophysin-immunofluorescent perikarya, particularly the ventral neuropil, which contains a dense network of dendrite-like processes extending from the vasopressin and oxytocin neurons of the NSO (Armstrong et al., 1982; Yulis et al., 1984). These processes form a bundle that is sandwiched between the magnocellular perikarya of the NSO and a thin glial cushion that, along with the basal lamina, makes up the ventral surface of the brain. A high density of synaptic contacts (Armstrong et al., 1982) and catecholamine varicosities (McNeill and Sladek, 1980) within the ventral neuropil, as compared to that in the NSO (Leranth et al., 1975), suggests that much of the synaptic input to the cells of the NSO is mediated by contacts within the ventral neuropil. Many of the presynaptic terminals found contacting these processes contain round, clear vesicles similar to cholinergic endings (Yulis et al., 1984).

A similar pattern of binding was apparent in the NC and NPV. The small groups of magnocellular neurons making up the NC contain either vasopressin or oxytocin (Rhodes et al., 1981) and are organized in a circular fashion around blood

vessels, with bundles of immunoreactive fibers following the vessel in the core of the nucleus. The present data helped to establish the NC as a possible primary target for cholinergic control of vasopressin/oxytocin secretion. The magnocellular neurons of the NPV also bound ^{125}I-αBTX but appeared to have a lower density of sites than those of the NSO or NC. Again, though, binding was associated exclusively with the regions of the NPV that contained neurophysin-immunoreactive cell bodies.

The parvocellular vasopressin-containing cells of the NSC were a contrast to the magnocellular neurons of the NSO, NC and NPV. Although a relatively high concentration of binding sites was present in the region surrounding the NSC, little or no overlap with neurophysin-immunoreactive cell bodies was observed. Vasopressin fibers projecting dorsally from the NSC (Sofroniew and Weindl, 1978) or dendrites extending laterally from the ventral NSC (Stephan et al., 1981; van den Pol, 1980) could be a potential target for cholinergic input. Assessment of this possibility will require closer examination of the ^{125}I-αBTX binding site within this region. Some support for an interaction of a putative nicotinic cholinergic receptor with the NSC has been provided by the observation that αBTX, applied locally to the region of the NSC, blocks the effects of light or cholinergic stimulation on serotonin-*N*-acetyltransferase activity in the pineal (Zatz and Brownstein, 1981).

Within the rostral hypothalamus, the magnocellular, neuroendocrine cells of the NSO, NC, and NPV are associated with the highest density of high-affinity ^{125}I-αBTX binding sites. The reason for this association is presently unknown but may reflect input from a nicotinic cholinergic system that is thought to control the release of vasopressin. Our findings supplement the recent work of Mason (1985), which illustrates staining of the NSO with a monoclonal antibody to the alpha subunit of the nicotinic cholinergic receptor of electric eel. The hypothalamic neuroendocrine system may be a model system for the clarification of the significance of the αBTX binding site in brain, as well as for the understanding of the control of vasopressin secretion.

References

Armstrong, W. E., J. Scholer, and T. McNeill (1982) Immunocytochemical, golgi and electron microscopic characterization of putative dendrites in the ventral glial lamina of the rat supraoptic nucleus. Neuroscience *7:* 679–694.

Arnauld, E., M. Cirino, B. S. Layton, and L. P. Renaud (1983) Contrasting actions of amino acids, acetylcholine, noradrenaline and leucine enkephalin on the excitability of supraoptic vasopressin-secreting neurons. Neuroendocrinology *36:* 187–196.

Barker, J. L., J. W. Crayton, and R. A. Nicoll (1971) Noradrenaline and acetylcholine responses of supraoptic neurosecretory cells. J. Physiol. (Lond.) *218:* 19–32.

Betz, H., D. Graham, and H. Rehm (1982) Identification of polypeptides associated with a putative neuronal nicotinic acetylcholine receptor. J. Biol. Chem. *257:* 11,390–11,394.

Bioulac, B., O. Gaffori, M. Harris, and J.-D. Vincent (1978) Effects of acetylcholine, sodium glutamate and GABA on the discharge of supraoptic neurons in the rat. Brain Res. *154:* 159–162.

Block, G. A., and R. B. Billiar (1979) Immunologic similarities between the hypothalamic α-bungarotoxin receptor and the *Torpedo californica* nicotinic cholinergic receptor. Brain Res. *178:* 381–387.

Carbonetto, S. T., D. M. Fambrough, and K. J. Muller (1978) Non-equivalence of α-bungarotoxin receptors and acetylcholine receptors in chick sympathetic neurons. Proc. Natl. Acad. Sci. USA *75:* 1016–1020.

Chalazonitis, A., L. A. Greene, and M. Nirenberg (1974) Electrophysiological characteristics of chick embryo sympathetic neurons in dissociated cell culture. Brain Res. *68:* 235–252.

Cheng, Y.-C., and W. H. Prusoff (1973) Relationship between the inhibition constant (K_i) and the concentration of inhibitor which causes 50 percent inhibition (I_{50}) of an enzymatic reaction. Biochem. Pharmacol. *22:* 3099–3108.

Chou, T. C., and C. T. Lee (1969) Effect of whole and fractionated cobra venom on sympathetic ganglionic transmission. Eur. J. Pharmacol. *8:* 326–330.

Conti-Tronconi, B. M., S. M. J. Dunn, E. A. Barnard, J. O. Dolly, F. A. Lai, N. Ray, and M. Raftery (1985) Brain and muscle nicotinic acetylcholine receptors are different but homologous proteins. Proc. Natl. Acad. Sci. USA *82:* 5208–5212.

Dolly, J. O., and E. A. Barnard (1984) Nicotinic acetylcholine receptors: An overview. Biochem. Pharmacol. *33:* 841–858.

Duggan, A. W., J. G. Hall, and C. Y. Lee (1976) Alpha-bungarotoxin, cobra neurotoxin and excitation of Renshaw cells by acetylcholine. Brain Res. *107:* 166–170.

Gahwiler, B. H., and J. J. Dreifuss (1980) Transition from random to phasic firing induced in neurons cultured from the hypothalamic supraoptic area. Brain Res. *193:* 415–425.

Greene, L. A., A. J. Sytkowski, Z. Vogel, and M. Nirenberg (1973) α-Bungarotoxin used as a probe for acetylcholine receptors of cultured neurones. Nature *243:* 163–166.

Harden, T. K., R. B. Meeker, and M. W. Martin (1983) Interaction of a radiolabeled agonist with cardiac muscarinic cholinergic receptors. J. Pharmacol. Exp. Ther. *227:* 570–577.

Hayward, J. N., T. A. Reaves, Jr., R. S. Greenwood, and R. B. Meeker (1983) Neuroendocrine cells in vitro: Electrophysiology, triple labeling with dye marking, immunocytochemical and ultrastructural analysis and hormone release. In *Methods in Enzymology, Vol. 103, Hormone Action,* Pt. H, P. M. Conn, ed., pp. 132–147, Academic, New York.

Hunt, S. P., and J. Schmidt (1978a) The electron microscopic autoradiographic localization of α-bungarotoxin binding sites within the central nervous system of the rat. Brain Res. *142:* 152–159.

Hunt, S. P., and J. Schmidt (1978b) Some observations on the binding patterns of α-bungarotoxin in the central nervous system of the rat. Brain Res. *157:* 213–232.

König, J. F. R., and R. A. Klippel (1963) *The Rat Brain. A Stereotaxic Atlas of the Forebrain and Lower Parts of the Brain Stem.* Krieger, New York.

Lentz, T. L., and J. Chester (1977) Localization of acetylcholine receptors in central synapses. J. Cell Biol. *75:* 258–267.

Leranth, C., L. Zaborszky, J. Marton, and M. Palkovits (1975) Quantitative studies on the supraoptic nucleus in the rat. I. Synaptic organization. Exp. Brain Res. *22:* 509–523.

Lowry, O. H., N. H. Rosebrough, A. C. Farr, and R. J. Randall (1951) Protein measurement with Folin phenol reagent. J. Biol. Chem. *193:* 265–275.

Lowy, J., J. McGregor, J. Rosenstone, and J. Schmidt (1976) Solubilization of an α-bungarotoxin-binding component from rat brain. Biochemistry *15:* 1522–1527.

Lukas, R. J. (1984a) Properties of curaremimetic neurotoxin binding sites in the rat central nervous system. Biochemistry *23:* 1152–1160.

Lukas, R. J. (1984b) Detection of low affinity α-bungarotoxin binding sites in the rat central nervous system. Biochemistry *23:* 1160–1164.

Marks, M. J., and A. C. Collins (1982) Characterization of nicotinc binding in mouse brain and comparison with the binding of α-bungarotoxin and quinuclidinyl benzilate. Mol. Pharmacol. *22:* 554–564.

Marshall, L. M. (1981) Synaptic localization of α-bungarotoxin binding which blocks nicotinic transmission at frog sympathetic neurons. Proc. Natl. Acad. Sci. USA *78:* 1948–1952.

Mason, W. T. (1985) Staining of the magnocellular nuclei of the rat hypothalamus by a monoclonal antibody directed against the α-subunit of the nicotinic cholinergic receptor. Neurosci. Lett. *59:* 89–95.

McNeill, T. H., and J. R. Sladek, Jr. (1980) Simultaneous monoamine histofluorescence and neuropeptide immunocytochemistry: II. Correlative distribution of catecholamine varicosities and magnocellular neurosecretory neurons in the rat supraoptic and paraventricular nuclei. J. Comp. Neurol. *193:* 1023–1033.

Meeker, R. B., K. M. Michels, M. T. Libber, and J. N. Hayward (1984) Distribution of putative nicotinic cholinergic receptors within the supraoptic nucleus of the rat hypothalamus. Soc. Neurosci. Abstr. *10:* 89.

Mills, A., and S. Wonnacott (1984) Antibodies to nicotinic acetylcholine receptors used to probe the structural relationships between brain α-bungarotoxin binding sites and nicotinic receptors. Neurochem. Int. *6:* 249–257.

Morley, B. J. (1981) The properties of brain nicotine receptors. Pharmacol. Ther. *15:* 111–122.

Morley, B. J., J. F. Lorden, G. B. Brown, G. E. Kemp, and R. J. Bradley

(1977) Regional distribution of nicotinic acetylcholine receptor in rat brain. Brain Res. *134:* 161–166.

Morley, B. J., G. R. Farley, and E. Javel (1983) Nicotinic acetylcholine receptors in mammalian brain. TIPS *4:* 225–227.

Oswald, R. E., and J. A. Freeman (1981) Alpha-bungarotoxin binding and central nervous system nicotinic acetylcholine receptors. Neuroscience *6:* 1–14.

Patrick, J., and W. B. Stallcup (1977a) α-Bungarotoxin binding and cholinergic receptor function on a rat sympathetic nerve line. J. Biol. Chem. *252:* 8629–8633.

Patrick, J., and W. B. Stallcup (1977b) Immunological distinction between acetylcholine receptor and the α-bungarotoxin-binding component on sympathetic neurons. Proc. Natl. Acad. Sci. USA *74:* 4689–4692.

Polz-Tejera, G., J. Schmidt, and H. J. Karten (1975) Autoradiographic localisation of α-bungarotoxin binding sites in the central nervous system. Nature *258:* 349–351.

Reaves, T. A., Jr., A. Hou-Yu, E. A. Zimmerman, and J. N. Hayward (1983) Supraoptic neurons in the rat hypothalamo-neurohypophysial explant: Double labeling with lucifer yellow injection and immunocytochemical identification of vasopressin- and neurophysin-containing neuroendocrine cells. Neurosci. Lett. *37:* 137–142.

Rhodes, C. H., J. I. Morrell, and D. W. Pfaff (1981) Immunohistochemical analysis of magnocellular elements in rat hypothalamus: Distribution and number of cells containing neurophysin, oxytocin and vasopressin. J. Comp. Neurol. *198:* 45–64.

Romano, C., and A. Goldstein (1980) Stereospecific nicotine receptors on rat brain membranes. Science *210:* 647–650.

Sakai, K. K., B. H. Marks, J. M. George, and A. Koestner (1974) The isolated organ-cultured supraoptic nucleus as a neuropharmacological test system. J. Pharmacol. Exp. Ther. *190:* 482–491.

Salvaterra, P. M., and H. R. Mahler (1976) Nicotinic acetylcholine receptor from rat brain. J. Biol. Chem. *251:* 6327–6334.

Salvaterra, P. M., H. R. Mahler, and W. J. Moore (1975) Subcellular and regional distribution of ^{125}I-labeled α-bungarotoxin binding in rat brain and its relationship to acetylcholinesterase and choline acetyltransferase. J. Biol. Chem. *250:* 6469–6475.

Schmidt, J. (1977) Drug binding properties of an α-bungarotoxin-binding component from rat brain. Mol. Pharmacol. *13:* 283–290.

Schwartz, R. D., R. McGee, Jr., and K. J. Kellar (1982) Nicotinic cholinergic receptors labeled by [^{3}H]acetylcholine in rat brain. Mol. Pharmacol. *22:* 56–62.

Segal, M., Y. Dudai, and A. Amsterdam (1978) Distribution of an α-bungarotoxin-binding cholinergic nicotinic receptor in rat brain. Brain Res. *148:* 105–119.

Silver, J., and R. B. Billiar (1976) An autoradiographic analysis of [3H]α-bungarotoxin distribution in the rat brain after intraventricular injection. J. Cell Biol. *71:* 956–963.

Sladek, C. D. (1983) Regulation of vasopressin release by neurotransmitters, neuropeptides and osmotic stimuli. In *The Neurohypophysis: Structure, Function and Control, Progress in Brain Research,* Vol. 60, B. A. Cross and G. Leng, eds., pp. 71–90, Elsevier, New York.

Smolen, A. J. (1983) Specific binding of α-bungarotoxin to synaptic membranes in rat sympathetic ganglion: Computer best-fit analysis of electron microscope radioautographs. Brain Res. *289:* 177–188.

Sofroniew, M. V., and A. Weindl (1978) Projections from the parvocellular vasopressin- and neurophysin-containing neurons of the suprachiasmatic nucleus. Am. J. Anat. *153:* 391–430.

Sokol, H. W., E. A. Zimmerman, W. H. Sawyer, and A. G. Robinson (1976) The hypothalamic-neurohypophysial system of the rat: Localization and quantitation of neurophysin by light microscopic immunocytochemistry in normal rats and in brattleboro rats deficient in vasopressin and a neurophysin. Endocrinology *98:* 1176–1188.

Stephan, F. K., K. J. Berkley, and R. L. Moss (1981) Efferent connections of the rat suprachiasmatic nucleus. Neuroscience *6:* 2625–2641.

van den Pol, A. N. (1980) The hypothalamic suprachiasmatic nucleus of rat: Intrinsic anatomy. J. Comp. Neurol. *191:* 661–702.

Vogel, Z., G. J. Maloney, A. Ling, and M. P. Daniels (1977) Identification of synaptic acetylcholine receptor sites in retina with peroxidase-labeled α-bungarotoxin. Proc. Natl. Acad. Sci. USA *74:* 3268–3272.

Volle, R. L., and G. B. Koelle (1975) Ganglionic stimulating and blocking agents. In *The Pharmacological Basis of Therapeutics,* L. S. Goodman and A. Gilman, eds., pp. 565–574, Macmillan, New York.

Wang, G.-K., S. Molinaro, and J. Schmidt (1978) Ligand responses of α-bungarotoxin binding sites from skeletal muscle and optic lobe of the chick. J. Biol. Chem. *253:* 8507–8512.

Williams, M., and J. L. Robinson (1984) Binding of the nicotinic cholinergic antagonist, dihydro-β-erythroidine, to rat brain tissue. J. Neurosci. *4:* 2906–2911.

Yazulla, S., and J. Schmidt (1977) Two types of receptors for α-bungarotoxin in the synaptic layers of the pigeon retina. Brain Res. *138:* 45–57.

Yulis, C. R., B. Peruzzo, and E. M. Rodriquez (1984) Immunocytochemistry and ultrastructure of the neuropil located ventral to the rat supraoptic nucleus. Cell Tissue Res. *236:* 171–180.

Zatz, M., and M. J. Brownstein (1981) Injection of α-bungarotoxin near the suprachiasmatic nucleus blocks the effects of light on nocturnal pineal enzyme activity. Brain Res. *213:* 438–442.